SPECTRAL UNMIXING FOR PLANETARY EXPLORATION APPLIED TO CRISM/MRO HYPERSPECTRAL IMAGERY. F. Schmidt[1,2], X. Ceamanos[3], S. Douté[3], B. Luo[4], G. Jouannic[1,2,5] and J. Chanussot[4], [1]Univ Paris-Sud, Laboratoire IDES, UMR8148, Orsay, F-91405, France (frederic.schmidt@u-psud.fr); [2]CNRS, Orsay, F-91405, France [3]Laboratoire de Planétologie de Grenoble, CNRS/UJF, Grenoble, France [4]Gipsalab, Grenoble Institut of Technology, Grenoble, France [5]International Research School of Planetary Sciences, Università "G. d'Annunzio", Viale Pindaro 42, 65127 Pescara, Italy

Introduction: Visible and near infrared imaging spectroscopy is a key remote sensing technique to study planetary objects. Since their first appearance in 1989, spectral imagers have been onboard an increasing number of orbiters aimed at exploring our Solar System. They have been decisive when addressing important issues related to the surface or the atmosphere of Mars, Venus, Jupiter, Saturn, their moons and Titan. We propose to investigate the possible role of blind spectral unmixing techniques in efficiently and accurately analyzing planetary hyperspectral images without a priori knowledge. These recent methods assume a linear mixture of "pure" endmembers and estimate both the spectra **S** and the abundances **M**, knowing the hyperspectral image **X** in case of noise **e**:

$$\mathbf{X} = \mathbf{M} \cdot \mathbf{S} + \mathbf{e}$$

We will test these approaches using high spatial resolution imagery and geomorphological mapping techniques.

We selected the Russell dune on Mars because linear subpixel mixing is expected on CRISM data [1]. We built a geomorphological "ground truth" using the high spatial resolution of a HiRISE image (see fig. 1).

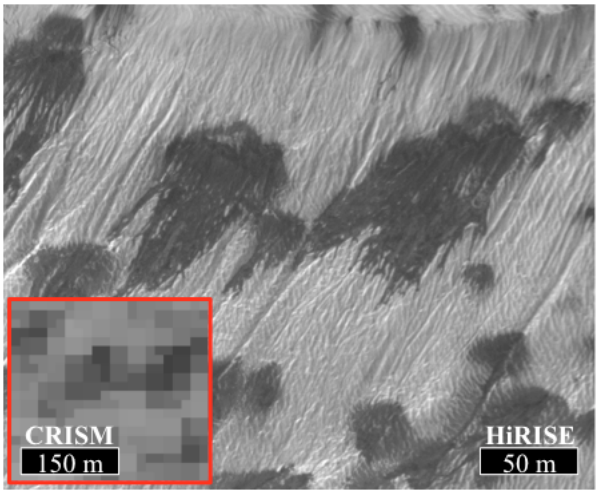

Fig. 1 Detail of HiRISE and CRISM image of the Russel Megadune.

Dataset: First, the HiRISE image [2] is classified into two classes, dark features and brighter ice, in order to generate a classification map. The classification is performed using a k-means strategy improved by manual operation in order to account for shadows and local photometric effects. Finally, only the spots and the elongated features are classified into the dark features class while the rest of the image - including shadows - is classified into the brighter ice class.

The CRISM/MRO [3] is treated by the following data pipeline: (i) artifact correction [4] (ii) spectral smile correction [5], (iii) photometric correction using an averaged incidence angle of 75°, (iv) atmosphere correction [6] and (v) estimation of the number of sources using Eigenvalue Likelihood Maximization (ELM) [7] (vi) blind source separation using Vertex Component Analysis (VCA) [ref VCA] and Bayesian Positive Source Separation (BPSS) [8,9,10].

The coregistration of HiRISE classification map and CRISM products are performed with the goal of identifying the group of HiRISE pixels that correspond to a given CRISM pixel. This is a quite challenging step because of the notable differences of spatial resolution of each instrument (~ 72 times larger for HiRISE). First, the selected CRISM channel is projected onto the HiRISE geographic space using the ancillary data, which provides the latitude and longitude of each pixel. We refine the registration by applying a spatial translation maximizing the correlation between the images. Finally, a Delaunay triangulation refines the registration by warping the CRISM image onto the HiRISE image using a set of manually selected ground control points. One should note that even though the coordinates of each CRISM pixel are available and the registration accuracy is sub-pixel level, some registration errors are expected.

The final step involves the transformation of the "ground truth" HiRISE classification map into an abundance map in the CRISM space. The abundance associated to each CRISM pixel is then calculated by counting the number of dark labels occurrences of each CRISM pixel and dividing the result by the total number of labels. The effect of point spread function is taken into account by a low pass filter.

Results : ELM estimates 6 endmembers. This is the only constraint we impose when applying VCA and BPSS on the CRISM image that went through the data pipeline. Figure 2 and 3 show the 6 spectra estimated for both methods.

Due to spectral non-linearity (for instance in the case of an intimate mixture) and residues from spectral

smile, atmospheric and photometric effects, the linear model can be degenerated and produce a splitting of physical sources (compounds with pure chemical composition) into a higher number of apparent endmembers due to the first order matrix **F**:

$$\mathbf{X} = \Im\left(\mathbf{M}\cdot\mathbf{S}\right) + \mathbf{e} \simeq \mathbf{F}\cdot\mathbf{M}\cdot\mathbf{S} + \mathbf{e}$$

We then argue on the spectral slope (residue of aerosols), albedo (characteristic of ice/dust), CO2 absorption bands (characteristic of ice) and identify three physical sources : dark dust, strong bright ice, weak bright ice (see fig. 2 and 3).

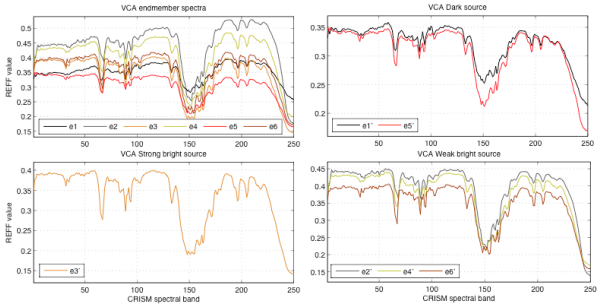

Fig 2: Top left: estimation of 6 sources using VCA algorithm. Top right: dark dusty materials. Bottom left: strong bright CO2 ice. Bottom left: weak CO2 ice.

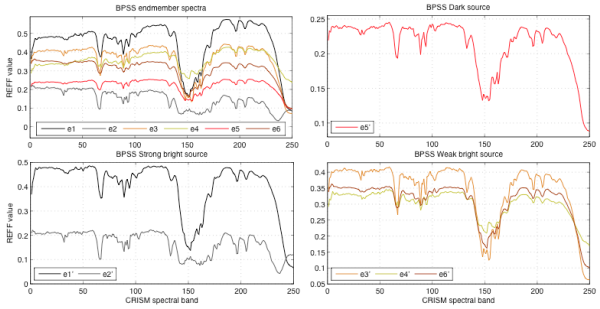

Fig 3: Same than fig. 2 but for BPSS algorithm.

Discussion: Figure 4 shows the results in a region with high confidence of coregistration. The "ground truth" derived from HiRISE classification and the abundance maps produced by the unmixing methods are compared and we find that the correlation coefficient is high, i.e.: 0.78 for VCA and 0.86 for BPSS. The absolute average error is 0.18 for VCA and 0.16 for BPSS. Due to local misregistration, the average correlation on all pixels is 0.54 for VCA and 0.57 for BPSS; the error is 0.17 and 0.1 respectively. We conclude that blind abundance maps have a satisfactory level of accuracy but the misregistration may limit their validation. Also non-linearity and residues have a strong influence on the extracted spectra.

In a future work, linear unmixing must be completed by the inversion of a physical model. It will consist to: (i) simulate the spectra of individual terrain units (physical source) with a radiative transfer algorithm (ii) estimate free parameters (dust content, surface properties, grain sizes) for all CRISM spectra using a priori information coming from the blind unmixing. For each pixel, the BPSS2 or VCA abundance values will be used as the most probable solution for the fractions while their uncertainty will give the width of the a priori distribution.

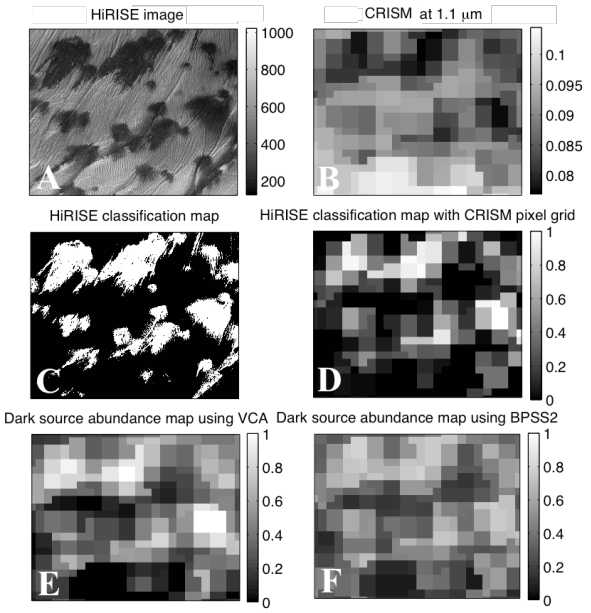

Fig4: (A) HiRISE image. (B) calibrated and coregistered CRISM image. (C) "ground truth" classification of dark feature (in white) (D) "ground truth" in the CRISM pixel grid. (E) blind estimation of dark dust using only CRISM data, analyzed by VCA (must be compared to D). (F) Same than (E) but for BPSS algorithm. In this figure, all images have the same scale than (A).

References: [1] Gardin et al., (2010), *JGR, 115*, E06, [2] A. S. McEwen et al., (2007), *JGR, 112*, E05S02 [3] S. Murchie et al. (2007), *JGR, 112*, E05, [4] M. Parente, (2008) *LPS IXXXX*, 2528 [5] X. Ceamanos and S. Douté, (2010), *IEEE TGRS*, 48, 3951, 3959 [6] S. Douté and X. Ceamanos, (2010) *IEEE WHISPERS* [7] B. Luo and J. Chanussot (2009*), IEEE ICIP* [8] S. Moussaoui et al., (2006) *IEEE TSP*, 54, 4133-4145 [9] N. Dobigeon et al. (2009) *IEEE SP*, 89, 2657-2669 [10] F. Schmidt et al. (2010) *IEEE TGRS*, 48, 4003-4013.